

Low Barrier Hydrogenolysis of the Carbon–Heteroatom Bond As Catalyzed by HAIF_4

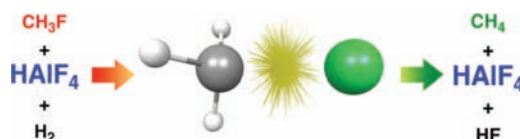
George Zhong, Bun Chan,* and Leo Radom*

School of Chemistry and Center of Excellence for Free Radical Chemistry and Biotechnology, University of Sydney, Sydney NSW 2006, Australia

chan_b@chem.usyd.edu.au; radom@chem.usyd.edu.au

Received December 8, 2008

ABSTRACT



Quantum chemistry calculations show that the barriers for HAIF_4 -catalyzed hydrogenolysis reactions of the carbon–heteroatom bond are reduced substantially compared with those for the uncatalyzed reactions. For example, the condensed-phase free-energy barrier for the HAIF_4 -catalyzed hydrogenolysis of CH_3F is about 130 kJ mol^{-1} , compared with 373 kJ mol^{-1} for the uncatalyzed reaction. The reactions are facilitated in the case of substrates that can give rise to a stable carbocation and for strongly acidic catalysts.

Hydrogenolysis describes the cleavage of a single bond A–B by molecular hydrogen, with the formation of two products A–H and B–H.¹ These reactions are frequently employed in organic synthesis,² industrial processes,³ and the removal of waste materials.⁴ In practice, most hydrogenolysis reactions are carried out in the presence of a transition-metal catalyst,⁵ with palladium being the most frequently employed.⁶ In contrast, transition-metal-free hydrogenolysis

reactions have received very little attention in previous experimental and theoretical investigations.

In an earlier study, the potential of HAIX_4 ($\text{X} = \text{F}, \text{Cl}, \text{Br}$) as a transition-metal-free catalyst for the hydrogenation of ethene was demonstrated.⁷ The study also included data indicative of AlX_3 as the first-ever transition-metal-free catalyst for hydrogenolysis reactions, although this was not commented on at the time. Using the reported energies, we find that the barrier for the hydrogenolysis of haloethanes is reduced by more than 300 kJ mol^{-1} in the presence of AlX_3 ! Such a striking result deserves further examination.

Although AlX_3 would not be a suitable catalyst for the hydrogenolysis of a general C–Y bond, i.e., when $\text{Y} \neq \text{X}$,⁸ HAIX_4 is a possible alternative.⁹ In the present study, we use quantum chemistry computations^{10,11} to probe the

(1) For a review of transfer-hydrogenolysis reactions, see: Rüchardt, C.; Gerst, M.; Ebenhoch, J. *Angew. Chem., Int. Ed. Engl.* **1997**, *36*, 1406.

(2) See, for example: (a) Greene, T. W.; Wuts, P. G. M. *Protective Groups in Organic Synthesis*; Wiley: New York, 1999. (b) Bolitt, V.; Mioskowski, C.; Kollah, R. O.; Manna, S.; Rajapaksa, D.; Falck, J. R. *J. Am. Chem. Soc.* **1991**, *113*, 6320. (c) Jennings, M. P.; Clemens, R. T. *Tetrahedron Lett.* **2005**, *46*, 2021. (d) Llàcer, E.; Romea, P.; Urf, F. *Tetrahedron Lett.* **2006**, *47*, 5815.

(3) See, for example: (a) Speight, J. G. *The Desulfurization of Heavy Oil and Residua*, 2nd ed.; Marcel Dekker: New York, 2000. (b) Grange, P. *Catal. Rev.* **1980**, *21*, 135. (c) Chianelli, R. R. *Catal. Rev.* **1982**, *26*, 361. (d) Poutsma, M. L. *Energy Fuels* **1990**, *4*, 113. (e) Startsev, A. N. *Russ. Chem. Rev.* **1992**, *61*, 175. (f) Ichimura, K.; Inoue, Y.; Yasumori, I. *Catal. Rev.* **1992**, *34*, 301.

(4) See, for example: (a) Zhanavskii, L. N.; Averyanov, V. A.; Treger, Y. A. *Russ. Chem. Rev.* **1996**, *65*, 617. (b) Lunin, V. V.; Lokteva, E. S. *Russ. Chem. Bull.* **1996**, *45*, 1519. (c) Pinder, A. R. *Synthesis* **1980**, 425. (d) Conventi, A.; Zilli, M.; De Faveri, D. M.; Ferraiolo, G. *J. Hazard. Mater.* **1991**, *27*, 127. (e) Hagh, B. F.; Allen, D. T. In *Innovative Hazardous Waste Treatment Technology*; Freeman, H. M., Ed.; Technomic: Lancaster, 1990; Vol. 1, p 45, and references cited therein.

(5) See, for example: (a) Sinfelt, J. H. *Catal. Rev.* **1970**, *3*, 175. (b) Sinfelt, J. H. *Catal. Lett.* **1991**, *9*, 159. (c) Urbano, F. J.; Marinas, J. M. *J. Mol. Catal. A* **2001**, *173*, 329. (d) Gormley, R. J.; Rao, V. U. S.; Soong, Y. *Appl. Catal. A* **1992**, *87*, 81. (e) Aizenberg, M.; Milstein, D. *J. Am. Chem. Soc.* **1995**, *117*, 8674. (f) Bianchini, C.; Meli, A. *J. Chem. Soc., Dalton Trans.* **1996**, 801. (g) McGrady, J. E.; Gracia, J. *J. Organomet. Chem.* **2005**, *690*, 5206, and references therein.

(6) King, A. O.; Larsen, R. D. In *Handbook of Organopalladium Chemistry for Organic Synthesis*; Negishi, E., Ed.; Wiley: New York, 2002.

(7) Senger, S.; Radom, L. *J. Phys. Chem. A* **2000**, *104*, 7375.

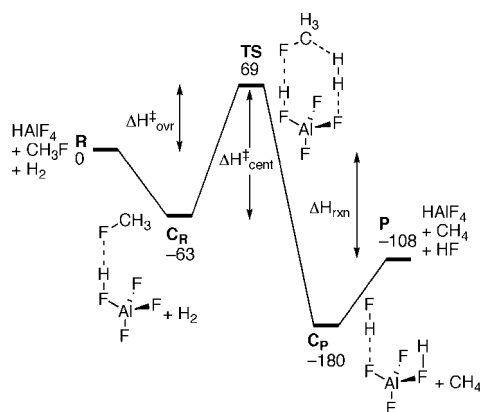
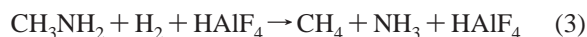
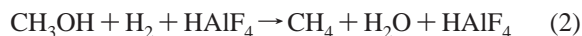


Figure 1. Schematic enthalpy profile (ΔH_{298} , kJ mol^{-1}) for the HAIF_4 -catalyzed hydrogenolysis of CH_3F

potential of HAIX_4 as a catalyst for hydrogenolysis reactions by examining the prototypical HAIF_4 -catalyzed hydrogenolysis reactions of CH_3F , CH_3OH , and CH_3NH_2 :



We have characterized concerted and stepwise pathways (Figure S1, Supporting Information) for reaction 1 and found that the concerted pathway is favored both in the gas phase and in solution. We therefore only discuss the concerted pathway in the present paper. A schematic enthalpy profile for the HAIF_4 -catalyzed hydrogenolysis of CH_3F (reaction 1) is displayed in Figure 1, while Table 1 compares uncatalyzed barriers (uncat) for all three reactions with the catalyzed overall (ovr) and central (cent) barriers (as defined

(8) AlX_3 is actually transformed to AlX_2Y during the reaction $\text{R}-\text{Y} + \text{H}_2 + \text{AlX}_3 \rightarrow \text{R}-\text{H} + \text{H}-\text{X} + \text{AlX}_2\text{Y}$.

(9) We are unaware of previous use of HAIX_4 , in particular, HAIF_4 , as a condensed-phase reagent. However, we anticipate that its acid/base properties would be similar to those for typical super acids such as HSbF_6 . Indeed, our preliminary calculations indicate that the gas-phase acidity of HAIF_4 ($1122.1 \text{ kJ mol}^{-1}$) is similar to that for HAsF_6 ($1112.2 \text{ kJ mol}^{-1}$).

(10) Performed using Gaussian 03 (ref 11). Electronic energies were obtained at the MP2/6-311+G(3df,2p)/B3-LYP/6-31+G(d,p) level, and thermal and entropy corrections used scaled B3-LYP/6-31+G(d,p) frequencies. Free energies of solvation were evaluated at the B3-LYP/6-31+G(d,p) level using the IEF-PCM model with UFF atomic radii and THF as the solvent.

(11) Gaussian 03, Revision D.02: Frisch, M. J.; Trucks, G. W.; Schlegel, H. B.; Scuseria, G. E.; Robb, M. A.; Cheeseman, J. R.; Montgomery, J. A., Jr.; Vreven, T.; Kudin, K. N.; Burant, J. C.; Millam, J. M.; Iyengar, S. S.; Tomasi, J.; Barone, V.; Mennucci, B.; Cossi, M.; Scalmani, G.; Rega, N.; Petersson, G. A.; Nakatsuji, H.; Hada, M.; Ehara, M.; Toyota, K.; Fukuda, R.; Hasegawa, J.; Ishida, M.; Nakajima, T.; Honda, Y.; Kato, O.; Nakai, H.; Klene, M.; Li, X.; Knox, J. E.; Hratchian, H. P.; Cross, J. B.; Bakken, V.; Adamo, C.; Jaramillo, J.; Gomperts, R.; Stratmann, R. E.; Yazyev, O.; Austin, A. J.; Cammi, R.; Pomelli, C.; Ochterski, J. W.; Ayala, P. Y.; Austin, A. J.; Cammi, R.; Pomelli, C.; Ochterski, J. W.; Ayala, P. Y.; Morokuma, K.; Voth, G. A.; Salvador, P.; Dannenberg, J. J.; Zakrzewski, V. G.; Dapprich, S.; Daniels, A. D.; Strain, M. C.; Farkas, O.; Malick, D. K.; Rabuck, A. D.; Raghavachari, K.; Foresman, J. B.; Ortiz, J. V.; Cui, Q.; Baboul, A. G.; Clifford, S.; Cioslowski, J.; Stefanov, B. B.; Liu, G.; Liashenko, A.; Piskorz, P.; Komaromi, I.; Martin, R. L.; Fox, D. J.; Keith, T.; Al-Laham, M. A.; Peng, C. Y.; Nanayakkara, A.; Challacombe, M.; Gill, P. M. W.; Johnson, B.; Chen, W.; Wong, M. W.; Gonzalez, C.; Pople, J. A. Gaussian, Inc.: Wallingford, CT, 2004.

Table 1. Gas-Phase Enthalpy (ΔH) and Condensed-Phase Free Energy (ΔG , Tetrahydrofuran, THF) Profiles for Reactions 1–3 (298 K, kJ mol^{-1}) (Upper Part of Table) and Uncatalyzed (uncat), Overall (ovr), and Central (cent) Enthalpy and Free Energy Barriers, and Reaction Energies (rxn) (298 K, kJ mol^{-1}) (Lower Part)^a

	ΔH , gas phase, 298 K			ΔG , THF, 298 K		
	1	2	3	1	2	3
R	0	0	0	0	0	0
C_R	-63	-105	-206	-8	-73	-193
TS	69	63	49	126	125	113
C_P	-180	-217	-277	-126	-216	-249
P	-108	-112	-104	-118	-122	-113
uncat	368	398	420	373	420	424
ovr	69	63	49	126	125	113
cent	132	168	255	134	198	306
rxn	-108	-112	-104	-118	-122	-113

^a See Figure 1 for definitions of stationary points, barriers, and reaction energy.

in Figure 1), as well as giving the reaction energies (rxn).¹² We find that the barriers for the uncatalyzed reactions are very high (greater than 360 kJ mol^{-1}) for all three substrates. However, the hydrogenolysis reactions are exothermic by more than 100 kJ mol^{-1} , and this opens up the opportunity for catalysis to reduce the barriers. Indeed, the overall enthalpic barriers are lowered substantially to less than 70 kJ mol^{-1} in the presence of the HAIF_4 catalyst.

We find that reactions 1–3 involve quite tightly bound complexes, and there is considerable variation in the binding energies. For the extreme case of reaction 3, we find that the complex **C_R** is essentially a strongly bound ion pair $[\text{NH}_3\text{CH}_3^+][\text{AlF}_4^-]$, and this leads to the central barrier being much higher than the overall barrier (Table 1).

Reactions 1–3 are formally termolecular processes, and this potentially carries a substantial entropic penalty. A closer examination of the relative entropic contribution to the free energies ($-T\Delta S$) and the relative free energies of solvation (ΔG_{solv} , tetrahydrofuran [THF] as solvent¹³) (Table 2) reveals that, while there are indeed substantial entropic penalties associated with formation of the **TS**, their impact on the central barriers is partially compensated by the entropic cost for the formation of the reactant complexes **C_R**. The entropic effect on **C_R** also leads to the complexes being less tightly bound. In addition, we find that, for reactions 1 and 2, stabilization of the **TS** by the solvent is greater than that for the corresponding complexes, presumably due to the larger carbocation character in the former. This further compensates for the entropic cost associated with assembling the **TS**. The

(12) Use of MP2/6-311+G(3df,2p) geometries leads to only minor changes in the energy profile of Figure 1, the largest change being just 1.4 kJ mol^{-1} for **C_R**.

(13) We have also investigated solvent effects using acetone ($\epsilon = 20.7$) as the solvent and found that the results are very similar to those obtained with THF ($\epsilon = 7.58$). Other continuum solvent models also produce similar qualitative results. We recognize that such solvents might be unstable under highly acidic conditions, but they are useful as theoretical models. In practice, stable and nonparticipating solvents such as ionic liquids might be more appropriate for such reaction conditions.

Table 2. Relative Entropic Contribution to Gas-Phase Free Energies ($-T\Delta S$) and Relative Free Energies of Solvation (ΔG_{solv}) for the Species Involved in Catalytic Hydrogenolysis Reactions 1–3 (298 K, kJ mol $^{-1}$)

	$-T\Delta S$			ΔG_{solv}		
	1	2	3	1	2	3
R	0	0	0	0	0	0
C_R	44	45	63	12	−12	−50
TS	81	86	99	−23	−23	−36
C_P	41	41	62	13	−41	−34
P	−2	−2	14	−8	−8	−24

bottom line is that we find that the central free-energy barriers in the condensed phase generally do not differ significantly from the corresponding gas-phase enthalpy barriers (Table 1). For reaction 3, the ion-pair complex **C_R** has a free energy of solvation that is higher than that for **TS**. This contributes to a substantially higher condensed-phase central barrier compared with the gas-phase reaction.

We now turn to the mechanism of the reactions. The transition structures for the uncatalyzed and HAIF_4 -catalyzed hydrogenolysis of CH_3F are shown in Figure 2 as prototypical examples for the reactions considered. We find a remarkable resemblance between these transition structures and those for nucleophilic substitution reactions (of H^- with CH_3F). Thus, the uncatalyzed **TS** (Figure 2a) is similar to that for the frontside $\text{S}_{\text{N}}2$ reaction (Figure 2b).¹⁴ On the other hand, in the catalytic hydrogenolysis of CH_3F , the **TS** (Figure 2c) may be regarded as backside attack on CH_3F by an H^- generated from H_2 , in a manner similar to a typical $\text{S}_{\text{N}}2$ reaction (Figure 2d).

The transition structure for the catalytic hydrogenolysis (Figure 2c) shows considerable carbocation character in the CH_3^+ moiety. For example, NBO charge calculations indicate that the CH_3 moiety in the transition structure bears a greater positive charge (+0.527) while the F leaving group bears a greater negative charge (−0.540) compared with corresponding values in the reactant, CH_3F (CH_3 : +0.437; F: −0.437). This hints at probable ways to improve the catalysis. Specifically, one might expect that substrates that give rise to a stabilized carbocation moiety in the **TS** might have lower catalytic hydrogenolysis barriers. Indeed, we find a lower overall gas-phase barrier (59 kJ mol $^{-1}$) for the catalytic hydrogenolysis of the C–F bond in $\text{NH}_2\text{CH}_2\text{F}$, where an NH_2CH_2^+ cation is formally involved in the transition structure, than the corresponding value for CH_3F (69 kJ mol $^{-1}$).

(14) See, for example: (a) Shaik, S. S.; Schlegel, H. B.; Wolfe, S. *Theoretical Aspects of Physical Organic Chemistry: The $\text{S}_{\text{N}}2$ Mechanism*; Wiley: New York, 1991; and references cited therein. (b) Harder, S.; Streitwieser, A.; Petty, J. T.; Schleyer, P. v. R. *J. Am. Chem. Soc.* **1995**, *117*, 3253.

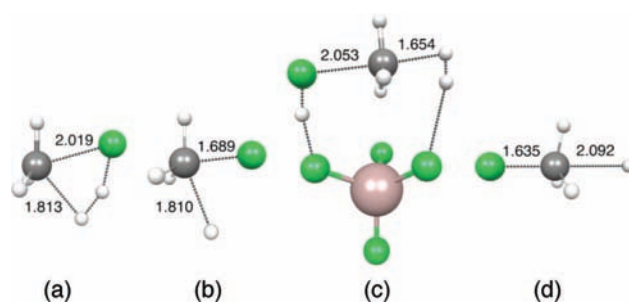


Figure 2. Transition structures and selected bond lengths (Å) for (a) the uncatalyzed hydrogenolysis of CH_3F , (b) frontside attack of CH_3F by H^- , (c) HAIF_4 -catalyzed hydrogenolysis of CH_3F , and (d) backside attack of CH_3F by H^- .

As the HAIF_4 catalyst acts as both an acid and a base catalyst, it is not immediately clear whether it is the acidic or basic component that is more important. Our calculations on the hydrogenolysis of CH_3F indicate that the more basic but less acidic catalyst $\text{HAI}(\text{NH}_2)_4$ leads to a considerably higher barrier (191 kJ mol $^{-1}$) than that for the corresponding HAIF_4 -catalyzed reaction (69 kJ mol $^{-1}$). This suggests that the acidity of the catalyst is a more important factor than its basicity in the catalysis.

In summary, the results of the present study demonstrate that HAIF_4 can be a very effective catalyst for hydrogenolysis, leading to reductions in overall barriers of approximately 300 kJ mol $^{-1}$. We find that the condensed phase hydrogenolysis of CH_3F has a central free-energy barrier of about 130 kJ mol $^{-1}$, and we hope that this result will encourage experimental studies. The hydrogenolysis transition structures are remarkably similar to those for frontside (uncatalyzed) and backside (catalyzed) nucleophilic substitution reactions. A systematic investigation of hydrogenolysis reactions involving a wide range of catalysts and substrates reinforces the present conclusions and will be reported elsewhere.

Acknowledgment. We gratefully acknowledge generous allocations of computing time from the NCI National Facility and ac3 and funding (to L.R.) from an ARC Discovery Grant and from the ARC Centre of Excellence for Free Radical Chemistry and Biotechnology.

Supporting Information Available: Details of theoretical procedures used, detailed structural and energy data, gas-phase enthalpy, and condensed-phase free energy profiles for reactions 1–3 and generalized concerted and stepwise mechanisms for the HAIX_4 -catalyzed hydrogenolysis of CH_3Y . This material is available free of charge via the Internet at <http://pubs.acs.org>.

OL802826H